

# Bioimaging assessment and effect of skin wound healing using bone-marrow-derived mesenchymal stromal cells with the artificial dermis in diabetic rats

## Hirokazu Inoue

Jichi Medical University  
Division of Organ Replacement Research  
Center for Molecular Medicine  
and  
Department of Orthopedics  
Tochigi 329-0498, Japan

## Takashi Murakami

Jichi Medical University  
Division of Organ Replacement Research  
Center for Molecular Medicine  
Tochigi 329-0498, Japan

## Takashi Ajiki

Jichi Medical University  
Division of Organ Replacement Research  
Center for Molecular Medicine  
and  
Department of Orthopedics  
Tochigi 329-0498, Japan

## Mayumi Hara

Jichi Medical University  
Division of Organ Replacement Research  
Center for Molecular Medicine  
Tochigi 329-0498, Japan

## Yuichi Hoshino

Jichi Medical University  
Department of Orthopedics  
Tochigi 329-0498, Japan

## Eiji Kobayashi

Jichi Medical University  
Division of Organ Replacement Research  
Center for Molecular Medicine  
Tochigi 329-0498, Japan

## 1 Introduction

Impaired wound healing represents a major clinical problem in patients with diabetes. The diabetic ulcer is a chronic and intractable injury, represents one of the most serious complications associated with diabetes, and is a leading cause of lower extremity amputation.<sup>1</sup> The lifetime risk of a person with diabetes developing a foot ulcer could be as high as 25%, and every 30 sec a lower limb is lost somewhere in the world as a consequence of diabetes.<sup>2</sup> Consequently, a novel strategy

**Abstract.** We investigate the relationship between the fate and healing effect of transplanted mesenchymal stromal cells (MSCs) in a rat diabetic skin wound model. Rats are treated with streptozotocin to induce diabetic conditions. A full-thickness skin defect is surgically made on the head of diabetic rats, and covered with an artificial dermis impregnated with either bone marrow cells (BMCs) or bone-marrow-derived MSCs from firefly luciferase (luc) transgenic (Tg) rats. Wound healing is evaluated using planimetry and immunohistochemistry, and the fate of transplanted MSCs is determined using *in-vivo* luminescent imaging. The diabetic wound treated with MSCs-impregnated artificial dermis is significantly smaller than that treated with artificial dermis alone at 1 week postoperation. Photons of luc+ MSCs are detected at the transplanted site during healing (3 weeks), whereas those of luc+ MSCs are depleted only after 1 week postimplantation. Immunohistochemistry at the healing site treated with MSCs demonstrates that CD31+ vessels increase with expression of vascular endothelial growth factor, suggesting that MSCs accelerate angiogenesis. These findings suggest that transplanted MSCs could be retained at wound sites during the healing process in a diabetic rat model, and subsequently promote wound healing through angiogenesis. © 2008 Society of Photo-Optical Instrumentation Engineers. [DOI: 10.1117/1.3042266]

Keywords: wound healing; mesenchymal stromal cell; angiogenesis; bone marrow cell; luminescence.

Paper 08130R received Apr. 20, 2008; revised manuscript received Sep. 14, 2008; accepted for publication Oct. 28, 2008; published online Dec. 18, 2008.

for the treatment of diabetic wounds is strongly needed to reduce clinical morbidity.<sup>3</sup>

Recently, attention has focused on cell therapy using bone-marrow-derived cells as a treatment of diabetic chronic wounds.<sup>3-5</sup> In fact, therapeutic trials involving bone marrow cells (BMCs) were clinically employed for the treatment of chronic wounds, including diabetic ulcers and decubitus.<sup>3,6,7</sup> Those studies demonstrated that BMCs play a critical role in angiogenesis and vasculogenesis for tissue repair,<sup>8</sup> and that bone-marrow-derived progenitor cells are recruited to peripheral tissues in response to ischemia.<sup>9</sup> In particular, BMCs include mesenchymal stromal cells [or mesenchymal stem cells

Address all Correspondence to: Eiji Kobayashi, M.D., Ph.D., Division of Organ Replacement Research, Center for Molecular Medicine, Jichi Medical University, Yakushiji 3311-1, Shimotsuke, Tochigi 329-0498 Japan. Tel: +81-285-58-7446; Fax: +81-285-44-5365; E-mail: eijikoba@jichi.ac.jp

(MSCs)], which have been shown to self-renew and differentiate into multilineage cells such as bone, cartilage, fat, myoblasts, vessels, and neurons.<sup>10-17</sup> Bone-marrow-derived MSCs possess a high expansion potential *ex vivo*, genetic stability, and can easily be isolated and transferred from the laboratory to the bedside. Thus, the clinical use of MSCs is of considerable interest in regenerative medicine.

While the use of MSCs offers insights into a new therapeutic approach concerning the repair of diabetic wounds, their fate following tissue implantation remains unclear. To determine the behavior of transplanted cells, an appropriate marker is essential in delineating the scientific basis of pre-clinical investigations. In this respect, firefly (*Photinus pyralis*) luciferase transgenic rats provide a stable internal light source for examining the behavior of transplanted cells in living rats. Moreover, the larger body size of the rat compared with the mouse allows for various surgical manipulations that may prove to have preclinical significance.

We demonstrate the relationship between the fate and role of bone-marrow-derived MSCs using topical transplantation of MSCs from luciferase transgenic rats to a diabetic skin wound. Our data showed that transplanted MSCs could be sufficiently retained during the healing period at wound sites, and that their retention was well correlated with improved wound healing. Immunohistochemistry also demonstrated that vascular endothelial growth factor and hypoxia-inducible factor 1 $\alpha$  were expressed at the healing site treated with MSCs. Thus, these results support the view that the use of bone-marrow-derived MSCs promotes diabetic wound healing through their long retention and expression of angiogenic factors.

## 2 Experimental Materials and Methods

### 2.1 Animals, Antibodies, and Reagents

Male Lewis (LEW) rats (250 to 280 g) were purchased from Charles River Japan, Incorporated (Yokohama, Japan). LacZ-Tg LEW rats (ROSA/LacZ-LEW)<sup>18,19</sup> and luciferase (luc)-Tg LEW rats (ROSA/Luciferase-LEW)<sup>20</sup> previously generated were used as donors (8 to 12 weeks old). All rats had free access to standard chow and drinking water, and were maintained on a 12-h light/dark cycle. All animal experiments in this study were performed in accordance with the Jichi Medical University Guide for Laboratory Animals.

Fluorescent isothiocyanate (FITC)-conjugated antirat CD29 monoclonal antibody (mAb, clone Ha2/5), (FITC)-conjugated antirat CD90 (Thy-1, clone HIS51) mAb, and phycoerythrin (PE)-conjugated antirat CD45 mAb (clone OX-1) were purchased from BD Pharmingen (San Diego, California). PE-conjugated antirat CD34 mAb (clone ICO115, sc-7324) was purchased from Santa Cruz Biotechnology (Santa Cruz, California). Isotype-matched IgG controls were purchased from BD Pharmingen. Mouse antivascular endothelial growth factor (VEGF) mAb (clone C1, sc-7269, Santa Cruz), rabbit anti-CD31 affinity-purified IgG (sc-1506-R, Santa Cruz), mouse IgG (sc-3879, Santa Cruz), and mouse antihypoxia inducible factor-1 $\alpha$  (HIF-1 $\alpha$ ) mAb (clone, H1alpha67, MAB5382, Chemicon, Temecula, California) were used as the primary Ab for immunohistochemistry, followed by biotinylated antirabbit (BA-1000) and antimouse IgG (BA-2001, Vector Laboratories, Burlingame, California), respectively.

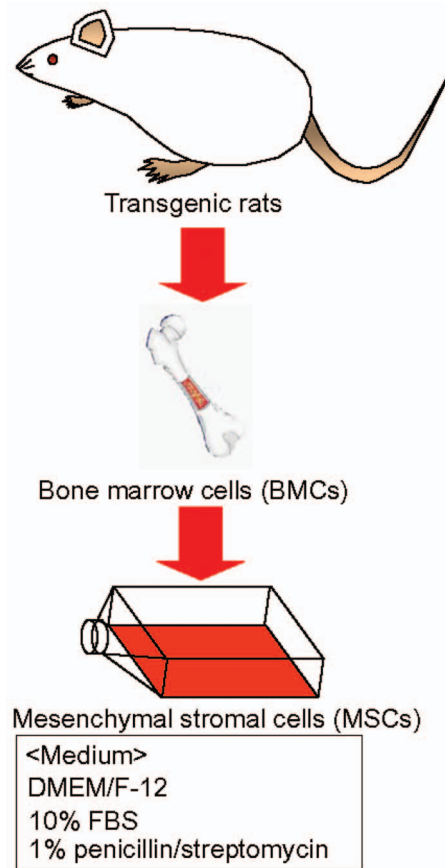


**Fig. 1** Schematic of mesenchymal stromal cells (MSCs) purification. Bone marrow cells (BMCs) were harvested by flushing femurs and tibiae with ice-cold PBS. Cells were cultivated in flasks containing DMEM/F-12 supplemented with 10% fetal bovine serum (FBS) and 1% penicillin/streptomycin.

Streptozotocin (STZ) was purchased from Wako Pure Chemicals (Osaka, Japan). Terudermis was used as an artificial dermis and kindly provided by Olympus Terumo Biomaterials Corporation (Tokyo, Japan).

### 2.2 Isolation and Culture of Mesenchymal Stromal Cells

Rat BMCs were harvested by flushing femurs and tibiae with ice-cold phosphate-buffered saline (PBS) as previously described.<sup>21</sup> Cells were filtered through a 70- $\mu$ m nylon mesh and plated in T75-cm<sup>2</sup> or T225-cm<sup>2</sup> flasks with DMEM/F-12 (Gibco, Grand Island, New York) supplemented with 10% fetal bovine serum (FBS) and 1% penicillin/streptomycin. The cultures were kept in a humidified atmosphere containing 5% CO<sub>2</sub> and 95% air at 37 °C. Nonadherent cells were removed after 24 h. Adherent cells were trypsinized with 0.25% trypsin-EDTA (Gibco), harvested, and then plated into new flasks at every 90% confluency. Adherent cells from passage 2 were frozen in liquid nitrogen for future use. Early passage cells were examined for their capacity to differentiate in culture (Fig. 1).

### 2.3 *In-Vitro Differentiation Assay*

Passage 4 MSCs were tested for their ability to differentiate into osteocytes and adipocytes. For adipocyte differentiation, cells ( $2 \times 10^5$ ) were cultured with Differentiation Media BulletKits-Adipogenic (Lonza, Basel, Switzerland) according to the manufacturer's instructions. MSCs were cultured in six-well plates with MSCs culture medium until they reached confluency. Cells were then exposed to three cycles of adipogenic induction media alternating with adipogenic maintenance media. Following three complete cycles of induction/maintenance, the MSCs were cultured for 7 more days in supplemented adipogenic maintenance medium. Cell differentiation to adipocytes was confirmed by Oil Red O (Muto Chemicals, Tokyo, Japan) staining. For osteogenic differentiation, cells ( $2 \times 10^4$ ) were plated, and the culture medium was replaced with Differentiation Media BulletKits-Osteogenic (Lonza) until confluence. Cells were stained with alizaline red S (Wako Pure Chemicals).

### 2.4 *Diabetic Wound Model and Cell Transplantation*

To induce diabetes mellitus, streptozotocin (STZ) in a 0.1-M citrate buffer (pH 4.3) was injected intravenously into the penile vein of normal LEW rats (60 mg/kg body weight). Rat blood glucose levels were then assessed using a glucometer after 3 days, and individual rats with glucose levels greater than 250 mg/dl were classified as diabetic and immediately utilized for further experimentation.

STZ-induced diabetic rats were anesthetized with pentobarbital (40 mg/kg) and full-thickness skin defects ( $2 \times 2$  cm) were made on the scalp.<sup>22</sup> Two hundred microliters of PBS containing fresh BMCs ( $1 \times 10^7$ ) or MSCs ( $1 \times 10^7$ ) was added to the inner layer of the same-sized artificial dermis for 30 sec at room temperature.<sup>23</sup> The wound was covered with the impregnated artificial dermis and sutured using 4-0 nylon. Artificial dermis impregnated with PBS was grafted onto rats that formed the control group.

The wounds were photographed every week in a standard prone position, and were monitored by planimetry using Scion image software (Scion Image Alpha 4.0.3.2, Scion Corporation, Maryland). The percent of wound area was calculated as the ratio of the nonhealing wound area to the original wound area.

### 2.5 *In-Vivo Bioluminescent Imaging*

*In-vivo* luminescent imaging was obtained using the noninvasive bioimaging system IVIS™ (Xenogen, Alameda, California) and analyzed using Igor (WaveMetrics, Lake Oswego, Oregon) and IVIS Living Image (Xenogen) software packages. To detect luminescence from luciferase-expressing cells, D-luciferin (potassium salt, Biosynth, Postfach, Switzerland) was injected intravenously into the penile vein or subcutaneously into the head skin of rats anesthetized (30-mg/kg body weight) with isoflurane. The signal intensity was quantified as photons flux in units of photons/sec/cm<sup>2</sup>/steradian in the region of interest.

### 2.6 *X-Gal Staining and Immunohistochemistry*

Rats were euthanized and the systemic circulation was flushed through the left ventricle with PBS followed by 4% paraformaldehyde (PFA). Specimens were divided and fixed in 4%

PFA, and embedded in either paraffin or Tissue Tec OCT Compound (Sakura Finetechnical Company, Limited, Tokyo, Japan). Thin sections (4 to 7  $\mu$ m) were stained with hematoxylin and eosin, or were used for immunohistochemistry.

To visualize lacZ expression, X-gal staining was performed as previously described.<sup>18</sup> Briefly, sections were washed three times with PBS containing 2-mM MgCl<sub>2</sub>, 0.01% sodium deoxycholate, and 0.02% Nonidet-P40. Specimens were treated with a  $\beta$ -gal staining solution (1 mg/ml of 5-bromo-4-chloro-3-indolyl-b-D-galactopyranoside, 2-mM MgCl<sub>2</sub>, 5-mM potassium hexacyanoferrate [III], and 5-mM potassium hexacyanoferrate [II] trihydrate) at 37 °C for 1 to 2 h.

For immunohistochemistry, sections were probed with anti-CD31, anti-VEGF, and anti-HIF-1 $\alpha$  antibodies. Specimens were blocked with 1% BSA in PBS and incubated overnight at 4 °C with anti-CD31 (diluted 1:50, 4  $\mu$ g/ml), anti-VEGF (diluted 1:100, 100  $\mu$ g/ml), and anti-HIF-1 $\alpha$  antibody (diluted 1:200, 5  $\mu$ g/ml), in 0.1% BSA, respectively. Biotinylated antirabbit IgG (Vector Laboratories, Burlingame, California) or biotinylated antimouse IgG (Vector Laboratories) was used as the secondary antibody (diluted 1:200 in 0.1% BSA for 1 h at room temperature). The labeled sections were incubated with horseradish peroxidase (HRP)-conjugated streptavidin (Vector Laboratories), and followed by diaminobenzidine (0.5  $\mu$ g/ml) for color visualization. Specimens were counterstained with hematoxylin. In sections stained with anti-CD31 antibody, CD31-positive tubular structures within the wound were considered as blood vessels. In ten similar sections, CD31-positive vessels were counted and normalized to 1 mm.<sup>24</sup>

### 2.7 *Statistical Analysis*

The Student's t-test, Tukey's HSD test, and U-test were used for the statistical analyses. The SPSS 11.0 system (SPSS Incorporated, Chicago, Illinois) was used for the statistical analysis. Differences between groups were considered significant when  $P < 0.05$ .

## 3 Results

### 3.1 *Characteristics of Bone-Marrow-Derived Mesenchymal Stromal Cells from Transgenic Rats*

To define the isolated MSCs from adult transgenic rats, the expression of cell surface markers was examined using FACS analysis [Fig. 2(a)]. As previously described,<sup>5,10</sup> isolated MSCs from lacZ-transgenic rats<sup>18,19</sup> were CD29 and CD90 (Thy-1) positive, and CD34 and CD45 negative. Moreover, the MSCs rapidly proliferated, formed colonies, and retained an adherent spindle-shaped morphology [Fig. 2(b)]. These cells were capable of differentiating into adipocytes [Fig. 2(c)] and osteocytes [Fig. 2(d)]. All of these phenotypes were equivalent to those of wild-type rats, and remained unchanged even in luciferase transgenic rats (data not shown). Thus, these results demonstrate that MSCs from transgenic rats possess appropriate differentiation potential. To avoid loss of multipotentiality for differentiation through passage in culture, MSCs derived from no more than a fourth passage were used for all experiments.



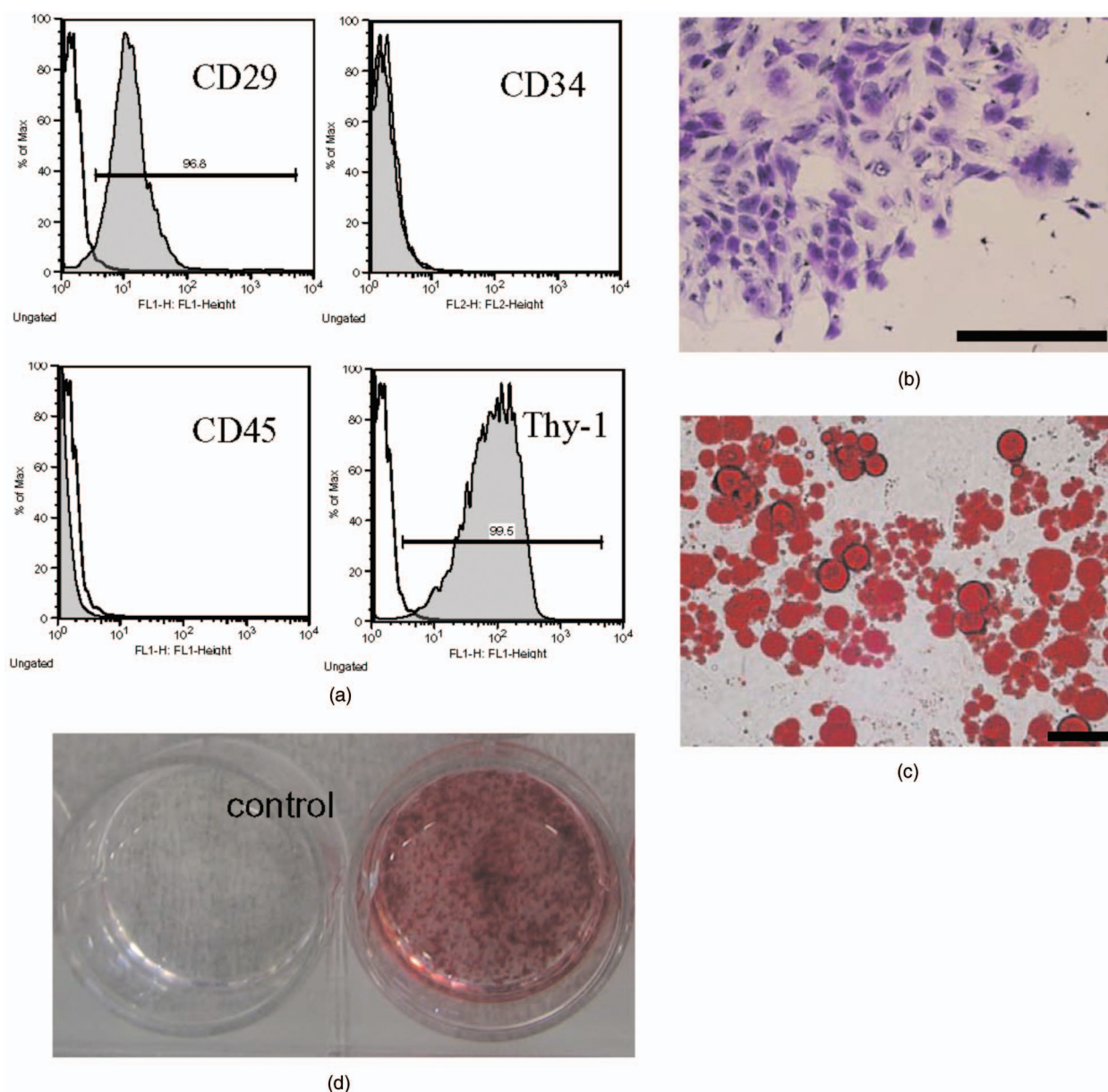


**Fig. 2** Characteristics of MSCs. (a) Flow cytometric histogram analysis of culture-expanded MSCs was performed as detailed in Sec. 2. Expression profiles for CD29, CD34, CD45, and Thy-1 are depicted. Cells were uniformly negative for CD34 and CD45, and positive for CD29, Thy-1 markers associated with MSCs. Specific antibody profile (gray) versus isotype-matched antibody control (black line) is shown. (b) Colony formation of MSCs from wild-type LEW rats. Colonies were stained with crystal violet. Adherent spindle-shaped cells proliferated to form colonies. Bar = 500  $\mu\text{m}$ . Under appropriate differentiation conditions, MSCs were capable of differentiating into (c) adipocytes (stained with Oil Red O for lipid droplets; Bar = 50  $\mu\text{m}$ ) and (d) osteocytes (stained with alizaline red for mineral deposition).

To visualize the fate of MSCs, luminescence sensitivity was examined in luc-Tg-derived MSCs. As shown in Fig. 3(a), at least  $5 \times 10^4$  MSCs from luc-Tg rats are required for substantial detection over the background *in vitro*, even though a linear dose-dependent output of light was maintained in the presence of D-luciferin. Although the MSCs comprised approximately 0.001% freshly isolated BMCs (data not shown), both expanded MSCs in culture and freshly isolated BMCs exhibited equivalent photon counts at the same cell number ( $1 \times 10^6$ ) [Fig. 3(b)].

### 3.2 Topical Administration of Mesenchymal Stromal Cells Promotes Skin Wound Healing in Diabetic Rats

To investigate whether skin wound healing could be impaired in the diabetic condition, streptozotocin (STZ) was intravenously injected into the penile vein of male rats, and full-thickness skin defects ( $2 \times 2$  cm) were then made on the scalp of diabetic rats (greater than 250 mg/dl of blood glucose). The skin defect was covered with an artificial dermis.

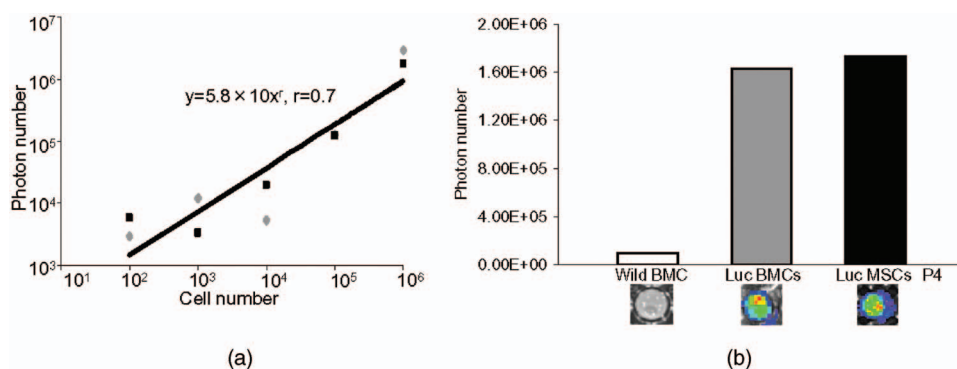


**Fig. 3** Characteristics of MSCs from luciferase Tg LEW rats. (a) Luciferase activity of MSCs from luciferase Tg LEW rats. MSCs from luciferase Tg LEW rats were plated onto 96-well plates at the indicated number. Luciferase activity (photon intensity) was evaluated in the presence of D-luciferin. Data represent the mean luciferase activity from two independent experiments (black squares and gray diamonds represent two different experimental trials). (b) Luciferase-expressing BMCs and MSCs possessed stronger luciferase activity than wild-type BMCs.

The wound area of diabetic rats was significantly smaller than that of control rats [Figs. 4(a) and 4(b)]. Skin wounds of control rats were almost totally restored at 3 weeks, while those of diabetic rats remained unhealed. These findings indicate impaired wound healing in diabetic rats.

In an effort to address the therapeutic effect of MSCs on skin wounds in diabetic rats, skin defects of diabetic rats were treated with either MSCs or BMCs that were impregnated

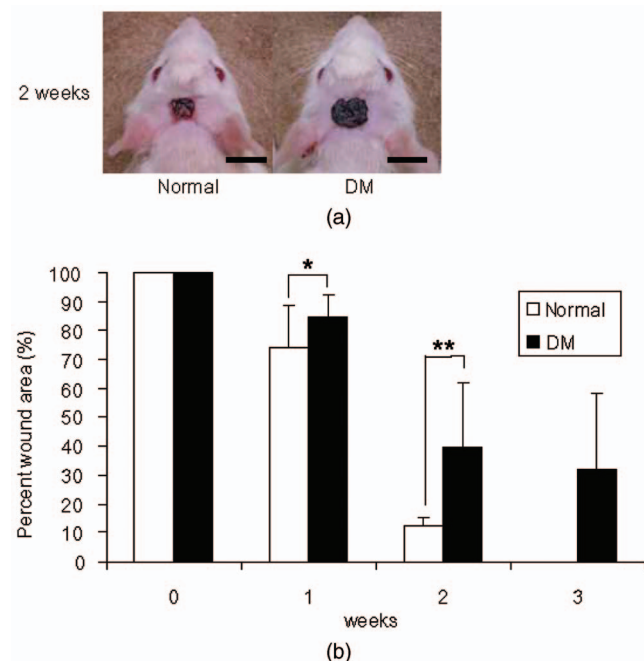


**Fig. 4** Delayed wound healing studies in rats. A square area (2 × 2 cm) was surgically excised down to muscle fascia on the head of streptozotocin (STZ)-induced diabetes mellitus (DM) LEW rats or normal LEW rats (n=22 animals in total). (a) The wounds were photographed every week, followed by planimetry analysis using Scion image software. Bar=1 cm. 1 and 2 weeks after the operation, DM rats healed significantly more slowly (b) than normal rats (\*p < 0.05 and \*\*p < 0.01, respectively). The skin wounds of normal rats were totally restored at 3 weeks. Data expressed as means ±SD. DM stands for streptozotocin-induced diabetes mellitus LEW rats. Normal is for normal LEW rats.

within an artificial dermis. Since an artificial dermis provides a scaffold for tissue regeneration and is amenable to impregnation with various cellular materials, it was used as a scaffold for the MSCs and BMCs. As shown in Figs. 5(a) and 5(b), the wound area of MSC-treated diabetic rats was strikingly smaller than that of BMC-treated diabetic rats 1 week after treatment. Notably, retention of MSCs and BMCs in the wound site was difficult without the artificial dermis (data not shown). These data demonstrate that topical administration of MSCs promotes skin wound healing in diabetic rats at an early stage. The artificial dermis promoted wound healing at 2 and 3 weeks after treatment, although the artificial dermis when used with BMCs or MSCs was not significantly smaller than when it was used alone.

### 3.3 Fate of Topically Administered Mesenchymal Stromal Cells on the Skin Wound of Diabetic Rats

To examine the fate of MSCs administered topically onto the wound area of diabetic rats, either MSCs or BMCs from luc-Tg rats were used as the therapeutic cell source with an artificial dermis. As shown in Fig. 6(a), MSC-derived photons were obtained during the whole period of wound healing (for 21 days), although photon counts decreased within a few days [to 40%, Fig. 5(b)]. BMC-derived photons decreased considerably to background levels within 7 days [Fig. 6(b)]. These results demonstrate that MSCs administered topically were retained to a greater extent than BMCs at the wound area of diabetic rats.

### 3.4 Mesenchymal Stromal Cells Accelerate Angiogenesis during Diabetic Wound Healing

Since the wound area of MSC-treated diabetic rats improved 1 week after treatment, specimens were stained with hematoxylin and eosin. As shown in Fig. 7(a), an increased number of vessel structures was observed in the MSC specimen, suggesting neoangiogenesis. Neoangiogenesis is a critical step in wound healing, and the CD31 molecule represents a major marker for vascular endothelial cells. Therefore, we set out to determine whether the administered MSCs affected the CD31-positive vessel number at the wound site of diabetic rats. In contrast with BMC treatment, MSC treatment showed that

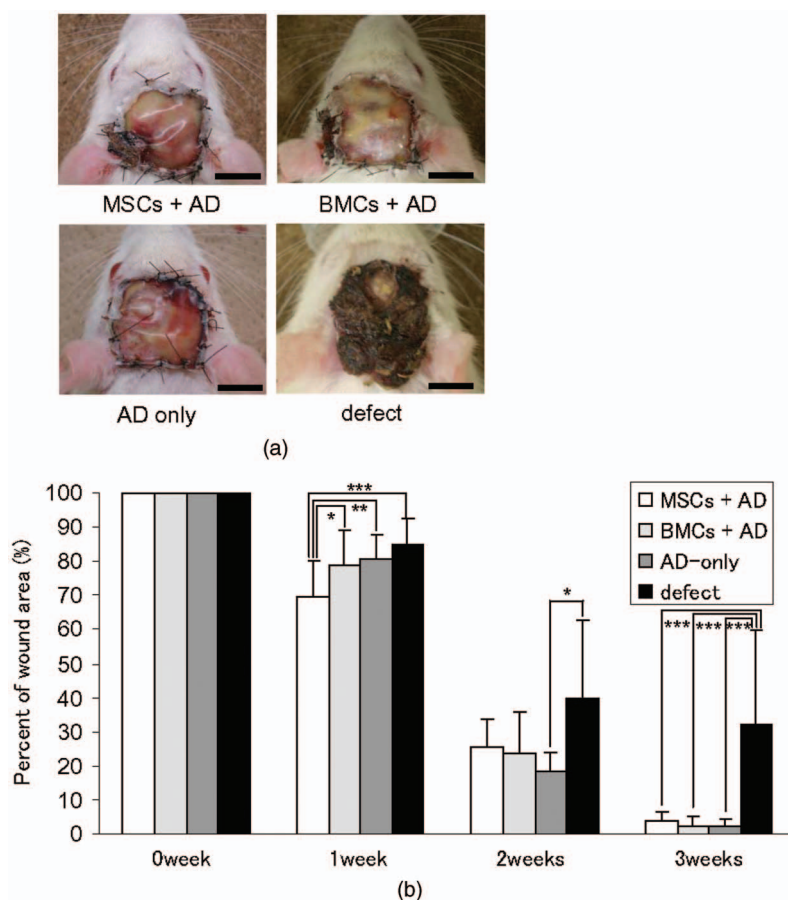


**Fig. 5** Healing effect of MSCs on diabetic wounds. (a) Groups comprising MSCs+artificial dermis (AD), BMCs+AD, AD-only, and defects were formed using DM rats ( $n=58$  animals in total) and photographed 1 week after transplantation. Bar=1 cm. (b) Percent of wound area was calculated using Scion image software, and values for the MSCs+AD group were significantly lower than those for the BMCs+AD, the AD-only and defect groups at 1 week after transplantation (\* $p<0.05$ , \*\* $p<0.01$ , and \*\*\* $p<0.001$ , respectively). Data expressed as means  $\pm$ SD.

CD31-positive adventitial vessels significantly increased in number at 1 week posttreatment ( $p<0.001$ ) [Fig. 7(a)]. Furthermore, MSCs from LacZ-Tg rats were used to assess the relationship between the presence of MSCs and vascular endothelial growth factor 1 (VEGF-1) expression using immunohistochemistry [Fig. 7(b)]. Specimens were stained using anti-VEGF antibodies and X-gal 1 week following cell transplantation. In comparison with BMC treatment, MSC transplantation increased VEGF expression with LacZ-expressing cells. Expression of hypoxia-inducible factor 1 $\alpha$  (HIF-1 $\alpha$ ), whose transcription factor tightly regulates VEGF expression under hypoxic conditions, was also well correlated with VEGF expression [Fig. 7(b)]. These results suggest that HIF-1-mediated VEGF expression contributes to the increased number of vessels at the wound site.

#### 4 Discussion

It has long been known that BMCs are mobilized during wound healing with inflammatory cells to orchestrate a cascade of tissue repair events.<sup>25</sup> Green fluorescent protein (GFP)-labeled bone marrow transplantation in wild-type mice allowed Badiavas et al. to demonstrate the participation of BMCs in cutaneous wound healing.<sup>26</sup> In this study, we demonstrated that the transplantation of MSCs enriched from

BMCs significantly decreased the wound area in a diabetic rat model, and that prolonged presence of MSCs was correlated with wound healing.

In addition to the differentiation potential, MSCs can easily be isolated and transferred from the laboratory to the bedside. Once expanded, MSCs in a culture from the patient could be stored under appropriate temperature conditions before use, and therefore MSCs from the same donor could be transplanted repeatedly.<sup>27</sup> Furthermore, recent advances in gene transfer technology also allow for transient or stable modification of MSCs (to produce a particular cytokine).<sup>28,29</sup> These attractive features of MSCs encourage the use of MSCs as therapeutic tools and for cell therapy. The presence of MSCs accelerated greater angiogenesis than BMCs, suggesting that MSCs are more effective than BMCs.

In this study, we used an artificial dermis to retain MSCs at wound sites. Artificial dermal substitutes are structurally optimized to incorporate the surrounding tissue and promote subsequent dermal remodeling.<sup>7,23</sup> Many types of dermal substitutes for wound coverage have been developed and are currently available.<sup>30-33</sup> Collagen matrix substitute dermis or artificial dermis is feasible for skin defects and is now commercially available for deep wounds, in which bones and/or tendons are exposed.<sup>30-32</sup> The use of an artificial der-



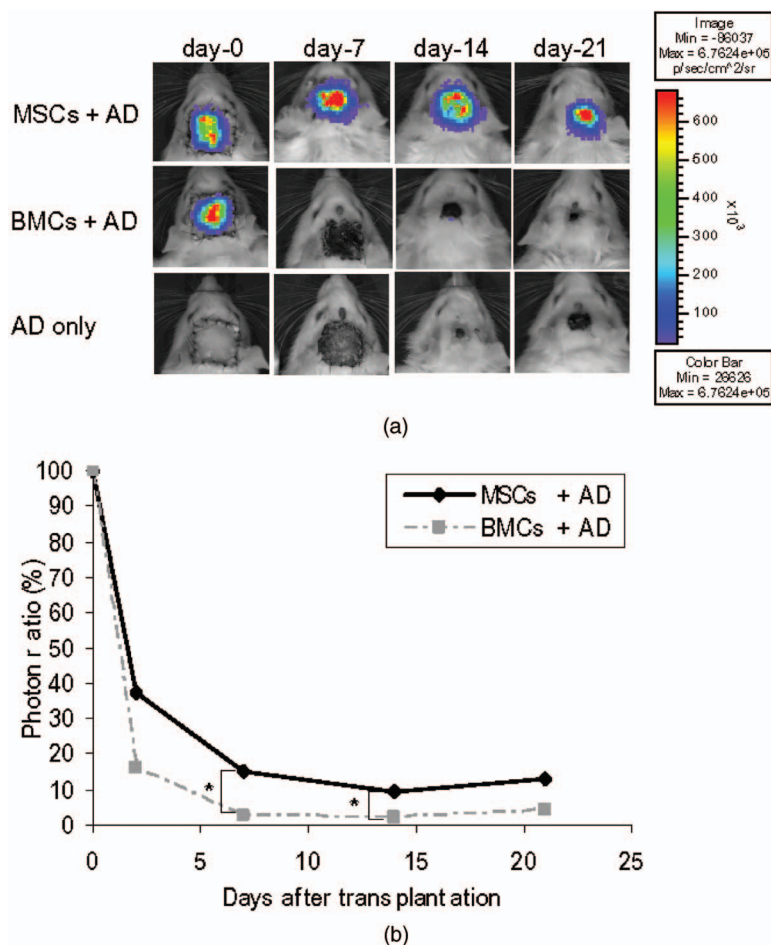


**Fig. 6** Transplantation of artificial dermis-impregnated luciferase-expressing bone-marrow-derived cells. Groups comprising MSCs+AD, BMCs+AD, and AD-only were formed using DM rats ( $n=15$  animals in total). D-luciferin was injected locally into the head skin of rats and luminescence was detected using the IVIS system. (a) Luminescence was recorded 0, 7, 14, and 21 days post-transplantation. (b) The time-course rate of luminescence is depicted. The MSCs+AD group had significantly higher luminescence than the BMCs+AD group (\* $p<0.05$ ).

mis provides a scaffold for tissue regeneration, in which sprouting capillaries and fibroblasts are capable of migrating into the collagen matrix. In this study, it was necessary for a scaffold to retain MSCs and BMCs in the wound site. The artificial dermis could easily be impregnated with various cellular material, and therefore their combination is expected to significantly improve the healing of chronic skin ulcers caused by ischemic disease, venous insufficiency, and diabetes.

*In vivo* luminescent imaging showed that prolonged retention of transplanted MSCs at the wound site was correlated with healing and an increased number of vessels. Prior to characterization being based on potential differentiation, MSCs were characterized based on criteria that included the ability to adhere to tissue culture plates, resemblance to fibroblasts *in vitro*, and colony formation.<sup>34</sup> Therefore, we assume that retention of MSCs at wound sites may be associated with their adhesion properties. In fact, Pittenger et al. demonstrated integrin expression with MSCs and noted the presence of alpha 1, alpha 2, alpha 3, alpha a, alpha v, beta 1, beta 3, and beta 4, together with other adhesion molecules such as ICAM-1, ICAM-3, VCAM-1, ALCAM, and endoglin/CD105.<sup>10</sup> Moreover, Ruster et al.<sup>35</sup> also demonstrated the ex-

pression of beta1 integrin VLA-4/CD49d on approximately 50% of the MSCs population present, and that MSCs are capable of rolling and adhering to cells that line blood vessels *in vitro* and *in vivo* in a P-selectin- and VLA-4/VCAM-1-dependent manner. Thus, the aforementioned supporting evidence allows us to speculate that the adhesion potential in MSCs can contribute to the observed retention at wound sites. In addition to the MSCs character, the improved wound healing associated with the use of MSCs may result from two possibilities. The first relates to the capacity of MSCs to secrete a variety of cytokines, which are relevant for tissue repair and regeneration.<sup>36-38</sup> These soluble mediators from implanted MSCs may complement early endogenous reactions that are involved in tissue repair, such as those involved in angiogenesis and extracellular matrix formation.<sup>39</sup> Treatment with MSCs resulted in enhanced expression of VEGF and an increased number of adventitial vessels, suggesting that MSCs contribute to angiogenesis. The second possibility may relate to the plasticity of MSCs to differentiate into a variety of cell types.<sup>23</sup> Since MSCs possess multidifferentiation potential, they may transdifferentiate into myoblasts and epithelium at the wound site.<sup>22,23</sup> However, the latter case is unlikely, since only a small number of transplanted MSCs were retained in

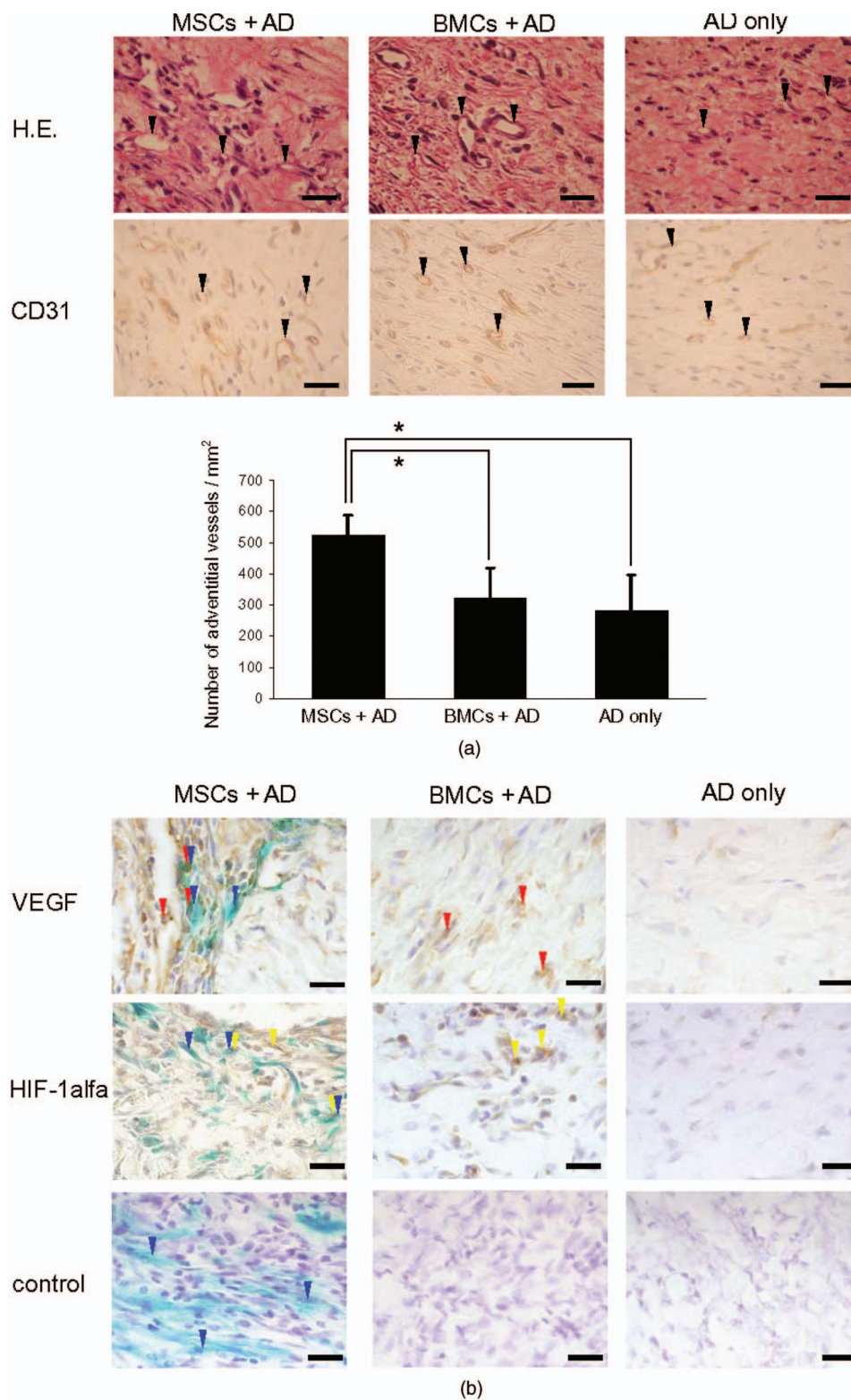


**Fig. 7** Transplantation of artificial dermis-impregnated LacZ-expressing bone-marrow-derived cells. (a): Upper panels show hematoxylin and eosin (HE) staining at 1 week after the transplantation, and lower panels show CD31 immunostaining. Bar=20  $\mu$ m. The MSCs+AD group had many microvessels (arrows) as shown by HE staining, and many CD31 positive vessels (arrows) as shown by CD31 immunostaining. The total vessel number was determined and expressed as vessel number/mm<sup>2</sup>. The MSCs+AD group had significantly more vessels than the BMCs+AD and AD-only groups (\* $p$ <0.001). Data expressed as means  $\pm$ SD. (b) Specimens were stained for VEGF (red arrows), HIF-1 $\alpha$  (yellow arrows), and mouse IgG (control) after X-gal staining (blue arrows). Bar=20  $\mu$ m. The MSCs+AD group expressed considerable levels of VEGF and HIF-1 $\alpha$ , and double-positive cells were identified.



the wound site, and MSC differentiation does not appear to be the major pathway for wound healing.

Since wound sites are relatively hypoxic, it was reasonable to record the expression of hypoxic condition-sensitive HIF-1 $\alpha$ .<sup>40</sup> HIF-1 $\alpha$  has been shown to stabilize and accumulate in cells under hypoxic conditions.<sup>41</sup> Interestingly, HIF-1 $\alpha$  expression with MSC treatment was more enhanced compared with the control [Fig. 7(b)]. There is the possibility that exogenous MSCs stabilize or up-regulate HIF-1 $\alpha$ , although this is difficult to determine due to the endogenous recruitment of MSCs.

In conclusion, the use of MSCs with an artificial dermis at an early stage could promote angiogenesis through MSC prolonged retention, and improve impaired wound healing in a diabetic rat model. To our knowledge, this is the first report to demonstrate the survival fate of transplanted MSCs in the diabetic condition, and to show that MSCs remained in the wound area, as determined by bioluminescent imaging. This preclinical model using MSCs provides an attractive strategy for cellular and scaffold therapies concerning intractable skin wounds such as diabetic wounds.

#### Acknowledgments

We would like to thank T. Yashiro, M. Kikuchi (Jichi Medical University), and all personnel in the Division of Organ Replacement Research, Center for Molecular Medicine, Jichi Medical University. We also wish to thank the Olympus Terumo Biomaterials Corporation for supplying the artificial dermis. This study was supported by grants from the Research on Health Sciences focusing on Drug Innovation program of the Japan Health Science Foundation (Kobayashi), and Research on Biological Resources (Murakami), Health of Labour Science Research Grants for Research from the Ministry of Health, Labour and Welfare, and the "High-Tech Research Center" Project for Private Universities: Matching fund subsidy from MEXT (Ministry of Education, Culture, Sports, Science, and Technology), 2002 to 2006. The transgenic rat embryos are available from the Health Science Research Resources Bank, National Bio Resource Project for the Rat, or Comparative Medicine Center and Research Animal Diagnostic Laboratory, College of Veterinary Medicine, University of Missouri, Missouri 65211.

#### References

1. N. Singh, D. G. Armstrong, and B. A. Lipsky, "Preventing foot ulcers in patients with diabetes," *JAMA, J. Am. Med. Assoc.* **293**(2), 217–228 (2005).
2. A. J. Boulton, L. Vileikyte, G. Ragnarson-Tennvall, and J. Apelqvist, "The global burden of diabetic foot disease," *Lancet* **366**(9498), 1719–1724 (2005).
3. Y. Yamaguchi et al., "Rapid healing of intractable diabetic foot ulcers with exposed bones following a novel therapy of exposing bone marrow cells and then grafting epidermal sheets," *Br. J. Dermatol.* **151**(5), 1019–1028 (2004).
4. Y. Wu, L. Chen, P. G. Scott, and E. E. Tredget, "Mesenchymal stem cells enhance wound healing through differentiation and angiogenesis," *Stem Cells* **25**(10), 2648–2659 (2007).
5. E. H. Javazon et al., "Enhanced epithelial gap closure and increased angiogenesis in wounds of diabetic mice treated with adult murine bone marrow stromal progenitor cells," *Wound Repair Regen* **15**(3), 350–359 (2007).
6. E. V. Badiavas and V. Falanga, "Treatment of chronic wounds with bone marrow-derived cells," *Arch. Dermatol.* **139**(4), 510–516 (2003).
7. S. Ichioka, S. Kouraba, N. Sekiya, N. Ohura, and T. Nakatsuka, "Bone marrow-impregnated collagen matrix for wound healing: experimental evaluation in a microcirculatory model of angiogenesis, and clinical experience," *Br. J. Plast. Surg.* **58**(8), 1124–1130 (2005).
8. V. Falanga, "Wound healing and its impairment in the diabetic foot," *Lancet* **366**(9498), 1736–1743 (2005).
9. Y. Misao et al., "Bone marrow-derived myocyte-like cells and regulation of repair-related cytokines after bone marrow cell transplantation," *Cardiovasc. Res.* **69**(2), 476–490 (2006).
10. M. F. Pittenger et al., "Multilineage potential of adult human mesenchymal stem cells," *Science* **284**(5411), 143–147 (1999).
11. M. B. Grant et al., "Adult hematopoietic stem cells provide functional hemangioblast activity during retinal neovascularization," *Nat. Med.* **8**(6), 607–612 (2002).
12. T. Asahara et al., "Isolation of putative progenitor endothelial cells for angiogenesis," *Science* **275**(5302), 964–967 (1997).
13. G. C. Kopen, D. J. Prockop, and D. G. Phinney, "Marrow stromal cells migrate throughout forebrain and cerebellum, and they differentiate into astrocytes after injection into neonatal mouse brains," *Proc. Natl. Acad. Sci. U.S.A.* **96**(19), 10711–10716 (1999).
14. K. W. Liechty et al., "Human mesenchymal stem cells engraft and demonstrate site-specific differentiation after in utero transplantation in sheep," *Nat. Med.* **6**(11), 1282–1286 (2000).
15. T. R. Brazelton, F. M. Rossi, G. I. Keshet, and H. M. Blau, "From marrow to brain: expression of neuronal phenotypes in adult mice," *Science* **290**(5497), 1775–1779 (2000).
16. E. Mezzer, K. J. Chandross, G. Harta, R. A. Maki, and S. R. Mckercher, "Turning blood into brain: cells bearing neuronal antigens generated in vivo from bone marrow," *Science* **290**(5497), 1779–1782 (2000).
17. D. Woodbury, E. J. Schwarz, D. J. Prockop, and I. B. Black, "Adult rat and human bone marrow stromal cells differentiate into neurons," *J. Neurosci. Res.* **61**(4), 364–370 (2000).
18. H. Inoue et al., "Development of new inbred transgenic strains of rats with LacZ or GFP," *Biochem. Biophys. Res. Commun.* **329**(1), 288–295 (2005).
19. T. Murakami and E. Kobayashi, "Color-engineered rats and luminescent LacZ imaging: a new platform to visualize biological processes," *J. Biomed. Opt.* **10**(4), 41204 (2005).
20. Y. Hakamata, T. Murakami, and E. Kobayashi, "Firefly rats as an organ/cellular source for long-term in vivo bioluminescent imaging," *Transplantation* **81**(8), 1179–1184 (2006).
21. M. Takahashi et al., "Establishment of lacZ-transgenic rats: a tool for regenerative research in myocardium," *Biochem. Biophys. Res. Commun.* **305**(4), 904–908 (2003).
22. Y. Yamaguchi et al., "Bone marrow cells differentiate into wound myofibroblasts and accelerate the healing of wounds with exposed bones when combined with an occlusive dressing," *Br. J. Dermatol.* **152**(4), 616–622 (2005).
23. H. Nakagawa, S. Akita, M. Fukui, T. Fujii, and K. Akino, "Human mesenchymal stem cells successfully improve skin-substitute wound healing," *Br. J. Dermatol.* **153**(1), 29–36 (2005).
24. H. Yamashita et al., "Vasohibin prevents arterial neointimal formation through angiogenesis inhibition," *Biochem. Biophys. Res. Commun.* **345**(3), 919–925 (2006).
25. R. Gillitzer and M. Goebeler, "Chemokines in cutaneous wound healing," *J. Leukoc. Biol.* **69**(4), 513–521 (2001).
26. E. V. Badiavas, M. Abedi, J. Butmarc, V. Falanga, and P. Quesenberry, "Participation of bone marrow derived cells in cutaneous wound healing," *J. Cell Physiol.* **196**(2), 245–250 (2003).
27. J. R. Mauney, V. Volloch, and D. L. Kaplan, "Role of adult mesenchymal stem cells in bone tissue engineering applications: current status and future prospects," *Tissue Eng.* **11**(5–6), 787–802 (2005).
28. M. Aluigi et al., "Nucleofection is an efficient nonviral transfection technique for human bone marrow-derived mesenchymal stem cells," *Stem Cells* **24**(2), 454–461 (2006).
29. L. Meinel et al., "Osteogenesis by human mesenchymal stem cells cultured on silk biomaterials: comparison of adenovirus mediated gene transfer and protein delivery of BMP-2," *Biomaterials* **27**(28), 4993–5002 (2006).
30. I. V. Yannas and J. F. Burke, "Design of an artificial skin. I. Basic design principles," *J. Biomed. Mater. Res.* **14**(1), 65–81 (1980).
31. R. Matsui, K. Osaki, J. Konishi, K. Ikegami, and M. Koide, "Evaluation of an artificial dermis full-thickness skin defect model in the rat," *Biomaterials* **17**(10), 989–994 (1996).

32. R. Matsui et al., "Histological evaluation of skin reconstruction using artificial dermis," *Biomaterials* **17**(10), 995–1000 (1996).
33. B. S. Atiyeh, S. N. Hayek, and S. W. Gunn, "New technologies for burn wound closure and healing--review of the literature," *Burns* **31**(8), 944–956 (2005).
34. A. J. Friedenstein et al., "Precursors for fibroblasts in different populations of hematopoietic cells as detected by the in vitro colony assay method," *Exp. Hematol.* **2**(2), 83–92 (1974).
35. B. Ruster et al., "Mesenchymal stem cells display coordinated rolling and adhesion behavior on endothelial cells," *Blood* **108**(12), 3938–3944 (2006).
36. M. Gnecci et al., "Evidence supporting paracrine hypothesis for Akt-modified mesenchymal stem cell-mediated cardiac protection and functional improvement," *FASEB J.* **20**(6), 661–669 (2006).
37. T. Kinnaird et al., "Marrow-derived stromal cells express genes encoding a broad spectrum of arteriogenic cytokines and promote in vitro and in vivo arteriogenesis through paracrine mechanisms," *Circ. Res.* **94**(5), 678–685 (2004).
38. T. Kinnaird et al., "Local delivery of marrow-derived stromal cells augments collateral perfusion through paracrine mechanisms," *Circulation* **109**(12), 1543–1549 (2004).
39. A. T. Badillo, R. A. Redden, L. Zhang, E. J. Doolin, and K. W. Liechty, "Treatment of diabetic wounds with fetal murine mesenchymal stromal cells enhances wound closure," *Cell Tissue Res.* **329**, 301–311 (2007).
40. H. H. Hassanain et al., "Smooth muscle cell expression of a constitutive active form of human Rac 1 accelerates cutaneous wound repair," *Surgery (St. Louis)* **137**(1), 92–101 (2005).
41. S. Salceda and J. Caro, "Hypoxia-inducible factor 1alpha (HIF-1alpha) protein is rapidly degraded by the ubiquitin-proteasome system under normoxic conditions. Its stabilization by hypoxia depends on redox-induced changes," *J. Biol. Chem.* **272**(36), 22642–22647 (1997).